

**UNIVERSIDAD DE CUENCA
FACULTAD DE INGENIERÍA
DEPARTAMENTO DE POSTGRADOS**

WRF SENSIBILITY TO MICROPHYSICS AND PLANETARY BOUNDARY LAYER AT
MICRO-CATCHMENT SCALE: THE CASE OF THE QUINUAS CATCHMENT IN THE
TROPICAL ANDES OF ECUADOR

**TRABAJO DE TITULACIÓN PREVIO A LA OBTENCIÓN DEL TÍTULO DE:
MAGÍSTER EN ECOHIDROLOGÍA**

AUTOR:

EDGAR CRISTÓBAL ALBUJA SILVA
C.I. 0105668834

DIRECTOR:

LENIN VLADIMIR CAMPOZANO PARRA
C.I. 0102677200

CO-DIRECTORES:

ESTÉBAN PATRICIO SAMANIEGO ALVARADO
C.I. 0102052594

ROLANDO ENRIQUE CÉLLERI ALVEAR
C.I. 0602794406

**CUENCA-ECUADOR
2018**



Abstract

Reliable high-resolution forecasts of precipitation are necessary to improve hydrological models forecasting. This is important in mountain regions, where complex convective and orographic processes occur. The present study evaluate the impact on precipitation, temperature and relative humidity forecasting of two sub-grid parameterization schemes: microphysics and planetary boundary layer (PBL). The results were compared for three resolutions (4km, 12 km and 36 km) in two nested domains. The Weather Research and Forecasting model was used. The analysis was based on two events of 20 and 15 mm cumulative rainfall during the dry and rainy seasons, respectively. Five allowable configurations were tested. The results show that microphysics and PBL's schemes perform satisfactory forecasts for the two seasons. Specifically, there is a dependence of the PBL for each season. The Thompson microphysics scheme showed good results on both events, resulting in an adequate configuration for Tropical Andean Mountains precipitation forecast. In addition, precipitation is highly sensitive to domain resolution. Moreover, forecasted temperature and relative humidity (RH) are also very sensitive to domain resolution: temperature forecast has lower performances as the domain gets finer, meanwhile RH and precipitation improve their forecast.

Keywords: WRF, climate, simulation, high resolution, precipitation, temperature, relative humidity, convective, microphysic, planetary boundary layer, PBL, Andes, Ecuador.

Resumen

Para mejorar la predicción de modelos hidrológicos, se necesitan pronósticos confiables de alta resolución de la precipitación. Esto es importante en las regiones montañosas, donde ocurren complejos procesos convectivos y orográficos. El presente estudio evalúa el impacto sobre la precipitación, la temperatura y la predicción de la humedad relativa de dos esquemas de parametrización de sub-red: microfísica y capa límite planetaria (PBL). Los resultados se compararon para tres resoluciones (4 km, 12 km y 36 km) en dos dominios anidados. Se utilizó el modelo de Previsión e investigación meteorológica. El análisis se basó en dos eventos de precipitación acumulada de 20 y 15 mm durante las estaciones seca y lluviosa, respectivamente. Cinco configuraciones permitidas fueron probadas. Los resultados muestran que la microfísica y los esquemas de PBL realizan pronósticos satisfactorios para las dos estaciones. Específicamente, existe una dependencia del PBL para cada temporada. El esquema de microfísica Thompson mostró buenos resultados en ambos eventos, lo que resultó en una configuración adecuada para el pronóstico de precipitación en las montañas andinas tropicales. Además, la precipitación es muy sensible a la resolución del dominio. Además, la temperatura pronosticada y la humedad relativa (HR) también son muy sensibles a la resolución del dominio: el pronóstico de temperatura tiene un rendimiento menor a medida que el dominio se vuelve más fino, mientras tanto, la HR y la precipitación mejoran su pronóstico.

Palabras Clave: WRF, simulación, clima, alta resolución, precipitación, temperatura, humedad relativa, convectivo, microfísica, capa límite planetaria, PBL, Andes, Ecuador.





Contenido

Abstract	2
Resumen	2
Contenido	4
Índice de Tablas	4
Índice de Figuras	4
1. Introduction	6
2. Materials	11
2.1. Study Area	11
2.2. Data	12
3. Methods	12
3.1. WRF setup	12
3.2. Case study periods	15
3.3. Skill metrics and analyses	15
4. Results and discussion	15
4.1. Sensitivity to the downscaling approach	15
4.2. Timing and development of simulated events	17
4.2.1 Simulation of precipitation	17
4.2.2 Simulation of temperature	20
4.2.3 Simulation of relative humidity	22
5. Conclusions	24
6. Acknowledges	25
7. References	25

Índice de Tablas

Table 1 Configurations for sensitivity study of subgrid parameterizations	14
---	----

Índice de Figuras

Figure 1 Study Area	11
Figure 2 Domain configuration for the WRF-ARW model	13
Figure 3 Box plots of Daily rainfall, temperature and Relative humidity on the Qinuas catchment	14
Figure 4 30/05/2016 event time series of precipitation, temperature and relative humidity, observed and downscaled by ND and 2W for D01, D02 and D03 from left to right	16



Figure 5 31/08/2015 event time series of precipitation, temperature and relative humidity, observed and downscaled by ND and 2W for D01, D02 and D03 from left to right 17

Figure 6 Precipitation time series for 30/05/2016 (left) and 31/08/2015 (right), for D01, D02 and D03 from top to bottom. 18

Figure 7 Cumulative precipitation time series for 30/05/2016 (left) and 31/08/2015 (right), for D01, D02 and D03 from top to bottom..... 19

Figure 8 Taylor plots for the precipitation on both events across the three domains (end of the arrow indicate domain resolution improvement)..... 20

Figure 9 Temperature time series for 30/05/2016 (left) and 31/08/2015 (right), for D01, D02 and D03 from top to bottom..... 21

Figure 10 Temperature Taylor Diagram for the configurations at each Domain (the arrows indicate the development of resolution). Left and right, 30/05/2016 and 31/08/2015 event. 22

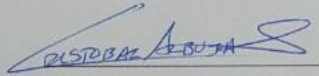
Figure 11 RH time series of WRF configurations vs Observed data..... 23

Figure 12 RH Taylor Diagram for the configurations at each Domain (the arrows indicate the develop of resolution) 24

Cláusula de Propiedad Intelectual

Edgar Cristóbal Albuja Silva, autor del trabajo de titulación "WRF sensibility to Microphysics and planetary boundary layer at micro-catchment scale: the case of the Quinuas catchment in the Tropical Andes of Ecuador", certifico que todas las ideas, opiniones y contenidos expuestos en la presente investigación son de exclusiva responsabilidad de su autor.

Cuenca, 28 de marzo de 2018

A handwritten signature in blue ink, appearing to read "EDGAR CRISTÓBAL ALBUJA SILVA".

Edgar Cristóbal Albuja Silva

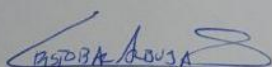
C.I. 0105668834

Cláusula de licencia y autorización para publicación en el Repositorio
Institucional

Edgar Cristóbal Albuja Silva en calidad de autor y titular de los derechos morales y patrimoniales del trabajo de titulación "WRF sensibility to Microphysics and planetary boundary layer at micro-catchment scale: the case of the Quinuas catchment in the Tropical Andes of Ecuador", de conformidad con el Art. 114 del CÓDIGO ORGÁNICO DE LA ECONOMÍA SOCIAL DE LOS CONOCIMIENTOS, CREATIVIDAD E INNOVACIÓN reconozco a favor de la Universidad de Cuenca una licencia gratuita, intransferible y no exclusiva para el uso no comercial de la obra, con fines estrictamente académicos.

Asimismo, autorizo a la Universidad de Cuenca para que realice la publicación de este trabajo de titulación en el repositorio institucional, de conformidad a lo dispuesto en el Art. 144 de la Ley Orgánica de Educación Superior.

Cuenca, 28 de marzo de 2018

A handwritten signature in blue ink, appearing to read 'Edgar Albuja Silva', written over a horizontal line.

Edgar Cristóbal Albuja Silva

C.I. 0105668834



1. Introduction

In conditions of climate change the increase of extreme precipitation events is expected, Allen [1] describe that changes due climate change will have large impacts on rainfall distributions and so on the hydrological cycles. This means we are likely to witness an increase in extreme precipitation events, which can trigger landslides, mud flows and floods. However risk prevention relies on the accuracy of rainfall forecasting, which it is still a challenge especially in mountain regions [2, 3]. This is especially urgent in developing countries where population grow makes land under high risk of flooding, potential areas of urbanization [4]. For instance the recent tragic event in Mocoa in Colombia occurred on the night hours. This flood was triggered by 130 mm of rain falling during a few hours. The Colombian town of Mocoa was hit by a powerful debris flow in the early hours of April 1, 2017 as overflowing rivers, mixed with vast amounts of rocks and soil, swept through the town. Colombia's National Risk Management Unit report 329 deaths, while 70 others officially remained listed as missing. Some 332 people were injured.

Precipitation is considered a key variable for understanding environmental variability and trends on catchments. Furthermore, it is one of the most important inputs in hydrological models [5]. Nevertheless, an estimation of the spatial distribution of precipitation based in scarce monitoring networks is inaccurate e.g. Thiessen averaging. In mountain regions such estimation is even more difficult due to the complex orography that induces processes such as rain shading, strong winds, and katabatic flows, among others, which increase the spatio temporal variability of rainfall. Some authors argue that precipitation can even hardly be represented from existing gridded precipitation data sets in mountainous regions with a dense gauging network [6, 7].

Thus, the use of Numerical Weather Prediction models (NWP) is becoming an important tool for spatial precipitation estimation and forecasting. These models can simulate longer periods of time e.g. years to decades, by successive model runs of shorter periods of time integration, from days to weeks. A good example of a NWP is given by Box et al. (2004) who used the Atmospheric Research Mesoscale Model MM5 for generating a contiguous multi-year weather data set for Greenland; they used a dynamical downscaling of 2.5° operational analyses from the European Centre for Medium-Range Weather Forecasts (ECMWF) by a sequence of daily model runs. With these results Box et al. (2006) used the MM5 output for driving a surface mass balance model of the Greenland Ice Sheet. NWP are also suitable for the dynamical downscaling of large-scale atmospheric variables. NWP can be initialized and laterally forced by assimilated observational data describing the large-scale atmospheric conditions throughout the simulation period. However some authors argue that NWP results depart from observations at finer spatial scales, but the use of some techniques such as nudging help to alleviate this drawback. The constantly improving capabilities of NWP offer the opportunity to provide precipitation fields among other meteorological variables at high spatial and temporal resolution.

The capacity of NWP representing rainfall in complex terrain is still discussed. Using horizontal spatial resolutions of less than 10 km has been a progressive and a substantial improvement [10–12], as it allows more accurate representation of rainfall in mountain regions. Zängl [13] shows that increased spatial resolutions in areas of complex terrain can be highly beneficial for simulating precipitation fields. However, higher spatial resolution does not automatically improve a NWP skill simulating precipitation in mountainous regions [14]. Scheel [15] and Ward [15] show low correlations between simulated products and observational data for precipitation and



other meteorological variables, even on daily scale. More importantly, the development of a sensitivity analysis of sub grid parameterizations on mountain regions may enhance the performance of climate and weather representation [17].

Few studies have been conducted on the Andes for the evaluation of downscaled precipitation. Buytaert [18] evaluated downscaled annual precipitation by the RCM PRECIS at $0.5^{\circ} \times 0.5^{\circ}$ resolution in Ecuador. Large errors were detected in RCM precipitation, sometimes larger than those obtained from GCMs. However the authors claim that the representation of precipitation gradients was improved. Such inconsistencies in mountain regions like the Andean Mountains, which often show elevation differences of 1 to 2 km within short distances of less than 10 km, may be attributed to atmospheric processes induced by the rather complex orography. Other studies have shown the strong control of orography and boundary-layer structure over precipitation on a river basin in Ecuador [19–21]. Ochoa [22], evaluated the representation of monthly precipitation in two basins of complex terrain in Ecuador using WRF from 1990-1999. The resolution in the inner domain was 12 km. They show that during the rainy seasons, precipitation was consistently overestimated, causing a strong systematic cold bias of temperature. At rainfall event scale Trachte [23] evaluated the mechanism for the formation of nocturnal convective clouds in the southern Ecuador on October 2009 on 4 different resolutions e.g. 36, 12, 4, 1 km, using the ARPS model. They demonstrated that only at 1km resolution the drainage of cold air was represented in the model, thus making possible the study of katabatic flows responsible for the formation of nocturnal convective rainfall in the escarpments of the Andes towards the Amazon.

In relation to the sub-grid parameterization of RCMs, it has been reported that the mixing of surface heat and moisture fluxes, into and outwards the atmospheric boundary layer is governed by the land surface model, the surface physics scheme and the planetary boundary layer (PBL) scheme, strongly influencing rainfall simulations [24]. Nakanishi [25] reported low biases for the local Mellor-Yamada Nakanishi and Niino (MYNN) Level 2.5 scheme, used in Japan and the Netherlands. Also, Ruizet al., (2010) reported that the non-local Yonsei University (YSU) scheme [27] represented better temperature, humidity and boundary layer height used in South America. On the other hand, the microphysics (MP) scheme is especially important because it is responsible for heat and moisture flux within the atmosphere and gives the surface resolved rainfall. For instance Rao [28] showed good results on forecasting heavy precipitation over India using the Ferrier scheme, whereas for the case of the Thompson scheme Rajeevan [29] obtained good agreement over south India simulating a heavy thunderstorm. These show the importance of conducting a detailed analysis of the different available schemes for the simulation of rainfall.

Thus, the aim of the present study was to assess the impact of two sub grid parameterization schemes in the representation of precipitation, temperature and relative humidity in a mountain region. The microphysics and planetary boundary layer (PBL) were studied by conducting a sensitivity study of five allowable configurations. Such evaluation was conducted in three spatial resolutions, i.e. 36, 12, 4 km using the Weather Research and Forecasting model (WRF). This study was conducted in the Quinuas Ecohydrological Observatory (QC), which is one of the best-monitored regions of the Andes at high altitudes, altitudinal range 3200 to 4500 m asl. The density of meteorological stations in the QC is 1 per 32 km², surpassing the recommended density of stations proposed by the World Meteorological Organization (WMO) which is 1 per 250 km² in mountain regions [19]. Therefore the event-wise evaluation of NWP, in complex terrain at micro catchment scale in the Andes is a novel contribution of this study.





2. Materials

2.1. Study Area

The QC is a páramo catchment of 94.1 km² located in the south of Ecuador (Figure 1), and is a sub-catchment of the Paute basin that drains towards the Amazon. It's located on the western Andean cordillera, oriented towards the east; thus, a strong influence from the Amazon is expected [21]. The elevation range of the basin is from 2700 to 4250 m asl. Part of the catchment lies within the Cajas National Park. The QC is fundamental for the region since it provides water for human consumption (for more than 600,000 inhabitants) as well as for downstream agricultural production,, industries, and hydropower generation.

The climate of the QC is mainly influenced by (i) continental air masses from the Amazon basin [30, 21], (ii) the Inter Tropical Convergence Zone ITCZ fluctuations, and (iii) fewer dry cool air masses from the west (Humboldt Current Influence). As a result the area has convective and orographic cloud formations and low temperatures (8.7°C daily mean) due to its elevation. The annual total precipitation varies from 1000 to 1500 mm. Rainfall seasonality is shown in Figure 1. The main rainy seasons February/May and October/November, are related to convective activity of the ITCZ displacement, whereas the precipitation during June/July is due to the enhancement of the easterlies during this season, therefore of advective nature [21].

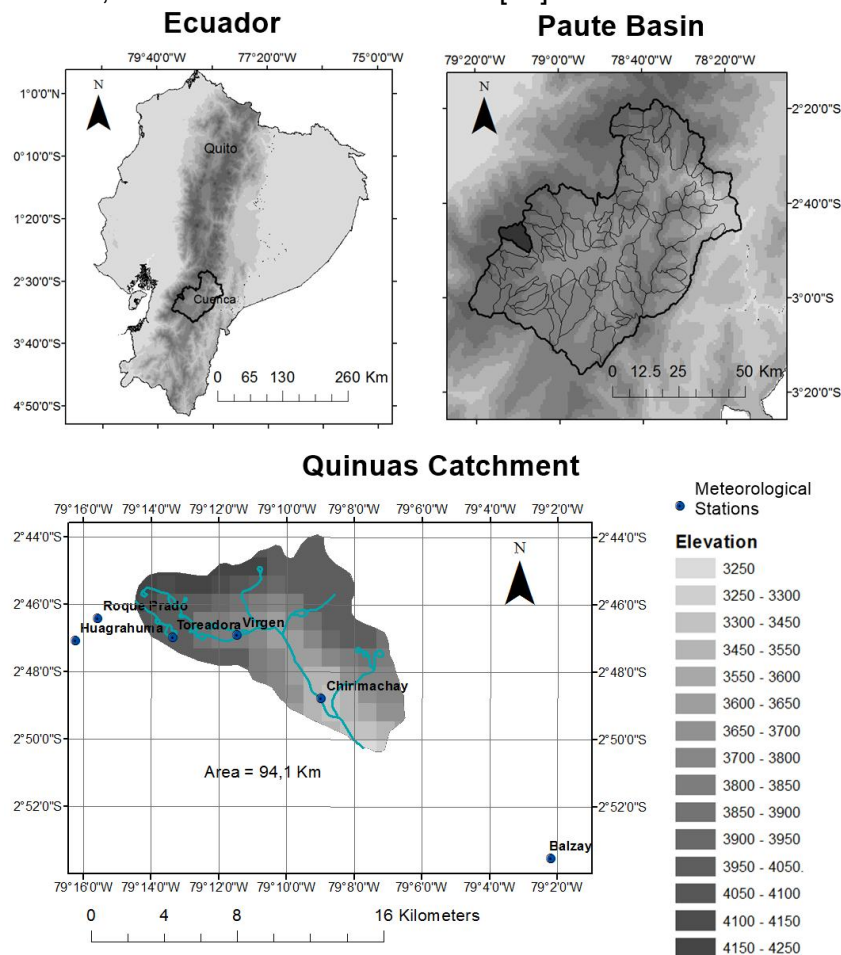


Figure 1 Study Area



2.2. Data

The WRF simulations were run using the three hourly data set from the global forecasted system database NCEP/GFS (GFS) from GFS Operation Model Global Tropospheric Analyses. It uses climate information from the surface, 32 pressure levels, and 4 sub-surface levels at a spatial resolution of 0.5°. GFS is available at <https://www.ncdc.noaa.gov/data-access/model-data/model-datasets/global-forecast-system-gfs>.

Model simulations for were assessed from meteorological stations located in the Quinuas Ecohydrological Observatory and surrounding areas, provided by the Department of Water Resources and Environmental Sciences of the University of Cuenca. The stations included in this dataset follow the recommendations of the World Meteorological Organization (WMO) for density on mountain regions [19], and data are quality-controlled. Rainfall data is recorded every 5 minutes and then aggregated to hourly data. Figure 3 shows the boxplots of daily precipitation, temperature and relative humidity by month, averaged over the ground stations in the study area.

The stations selected for this study followed two criteria: they must be located within the inner domain (D03), and must be situated above 2500 m asl. Data from four operational weather stations and two rain gauges fulfilled these criteria during simulation period. The weather stations are distributed over the altitudinal gradient. The location of the meteorological stations is shown in Figure 1. Complementarily, temperature and relative humidity data at 2m above the ground were used.

3. Methods

3.1. WRF setup

WRF version 3.7.1 with the dynamical core is used for the simulations, driven by GFS data. WRF is run in three domains (see Figure 2). The outer domain (D01) covers a wide area from northwestern South America into the Pacific Ocean heading south to northern Perú, with 36 km resolution. 50 grid-points in both directions x and y is used to capture large-scale processes and to avoid model artifacts near the lateral boundaries. The intermediate domain (D02) covers an area from southern Colombia to northern Peru with 12 km resolution and 82 by 82 points. The innermost domain (D03) includes the Paute Basin at 4 km spatial resolution with 112 by 112 grid points (Figure 2). The vertical structure of the atmosphere is modeled with 32 vertical layers. A lateral relaxation zone of 10 grid cells is used.

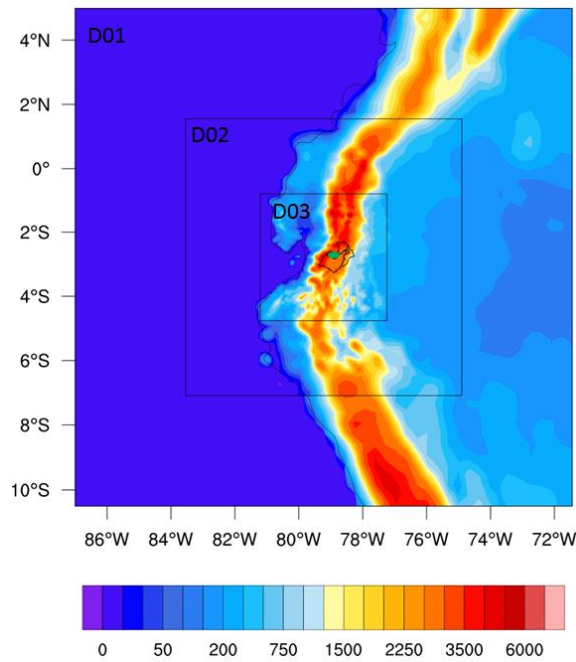


Figure 2 Domain configuration for the WRF-ARW model

In relation to the sub-grid parameterization schemes, Monin-Obukhov (MM5) surface physics scheme and an intermediate complexity land surface model (Noah LSM) are used. MM5 (Dudhia) and RRTM were used for the short wave and long wave radiation scheme respectively. These schemes are recommended for 1 to 4 km resolution cases in the ARW core for real cases. Due to the spatio-temporal complexity of rainfall in the QC, due to advective, convective and orographic components [21] the convective parameterization Kain-Fritsch [31] was set in the three domains.

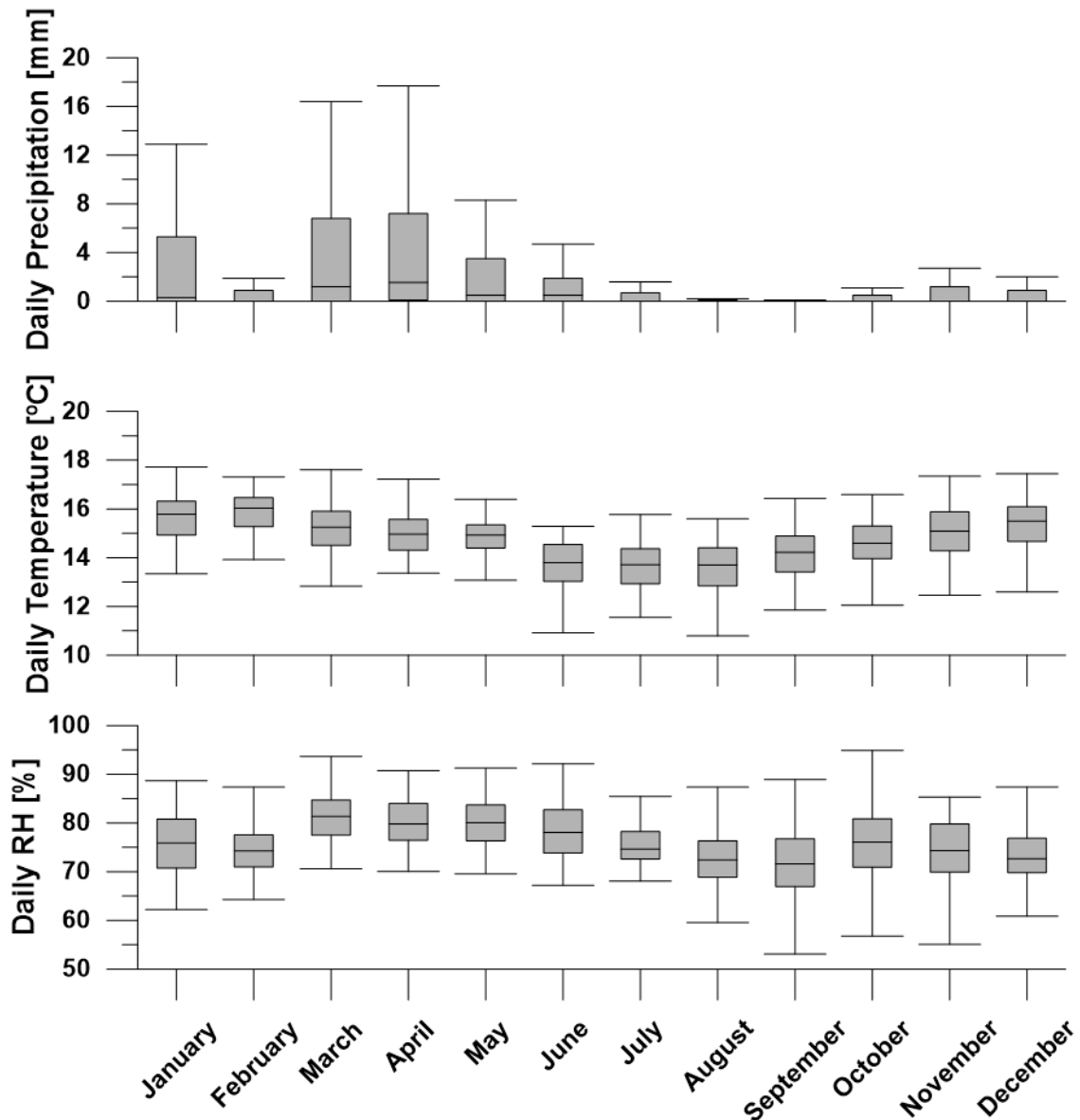


Figure 3 Box plots of Daily rainfall, temperature and Relative humidity on the Qinuas catchment.

For the sensitivity study of PBL parameterization, MYNN and YSU schemes are evaluated. With respect to the microphysics (MP) sensitivity analysis, three schemes are compared, (i) the WRF double moment 6-class scheme (WDM6), (ii) the Thompson scheme [29], and (iii) the Ferrier scheme [32]. Therefore, five allowable simulations are evaluated (see Table 1). The parameterization schemes were chosen based on literature review and in agreement with processes occurring in this region. All configurations were started with sea surface temperature and updated every six hours.

Table 1 Configurations for sensitivity study of subgrid parameterizations

Configuration	MP	PBL
C1	Thompson	YSU
C2	Thompson	MYNN
C3	Ferrier	YSU
C4	Ferrier	MYNN
C5	WSM6	YSU



The use of nesting enables the simulation of feedbacks among various meteorological processes occurring at various temporal and spatial scales. One-way nesting by NDOWN (ND) uses the output of a coarser grid simulation as input for the finer grid simulation. Two-way nesting, 2W, involves feedback from the fine domain to the coarse domain and vice versa. Some studies have shown that some methods of nesting can lead to more accurate predictions [33–36]. Therefore in order to make a more comprehensive evaluation, the results are compared for ND and 2W nesting approaches.

3.2. Case study periods

QC is located in the western part of the Paute basin. Due to orographic conditions, besides the influence of the ITCZ during February-May and October-November, during the dry season July-October the climatic influence prevails from the Amazon due to the eastward orientation to the easterlies [37]. Thus to consider different synoptic conditions, the analysis was based on two rainfall events, one in the dry and one in the rainy season, registering 15 and 20 mm of cumulative rainfall, in 48 hours and 60 hours respectively. The first event was simulated from 2015-08-31 19:00 to 2015-09-02 19:00 local time, and the second event from 2016-05-29 19:00 to 2016-06-02 12:00 local time. The first 6 hours were used for the spin-up of the model and discarded from the analysis.

3.3. Skill metrics and analyses

The sensitivity study attempts to quantify the overall skill of the model in the QC, thus the average of the six ground stations is evaluated for precipitation, temperature and relative humidity on an hourly basis. Taylor plots are used to evaluate the skill of the models. Taylor plots use the Pearson correlation, the centered root mean squared error and the standard deviation into one single graph [38], which provide a brief statistical outline of how well the configurations match the observations [12, 39, 40]. The configuration which has the largest correlation, smaller RMSE and comparable variance close to the observations will be the best among all [39]. In addition to the Taylor diagrams, the timing and the development of the event is qualitatively evaluated on the time series plots.

4. Results and discussion

4.1. Sensitivity to the downscaling approach

To evaluate the sensitivity to the downscaling approach, in Figure 4, ND and 2W (red line and blue line respectively) for the 30/05/2016 event, the precipitation, temperature and RH is presented for D01, D02 and D03.

In Figure 4 the simulated precipitation for 36 and 12 km resolution, ND and 2W similarly represent the observations. However for 4 km resolution ND strongly overestimate the precipitation. ND represents the simulated temperature for D01 better. However for D02 and D03 the results of both downscaling approaches are very



similar. It is interesting to observe that ND & 2W show a cold bias of ca. 2° in D02, and ca. 5° in D03. As noted by Roux [41] a negative bias in mountain regions can be influenced by local land surface and terrain conditions. For RH in D01 ND represents the observed data better. However for D02 & D03 both approaches are very similar. Thus for the 30/05/2016 event ND & 2W approaches present very similar results, although some improvements are shown by ND only on the 36 km resolution. Contrarily for the 4km resolution the 2W approach fits the observed precipitation better. Figure 5 shows the same results for the 31/08/2015 event. The simulated precipitation represented by the 2W approach is better. ND precipitation is underestimated in D01 and overestimated in D02. For temperature ND & 2W are very similar for D02 & D03 but ND strongly overestimates temperature in D01. The simulated RH is very similar for D02 & D03, despite underestimation of RH for D01. These results reflect that ND in D01 presents low relative humidity, leading to an underestimation of rainfall and overestimation of temperature.

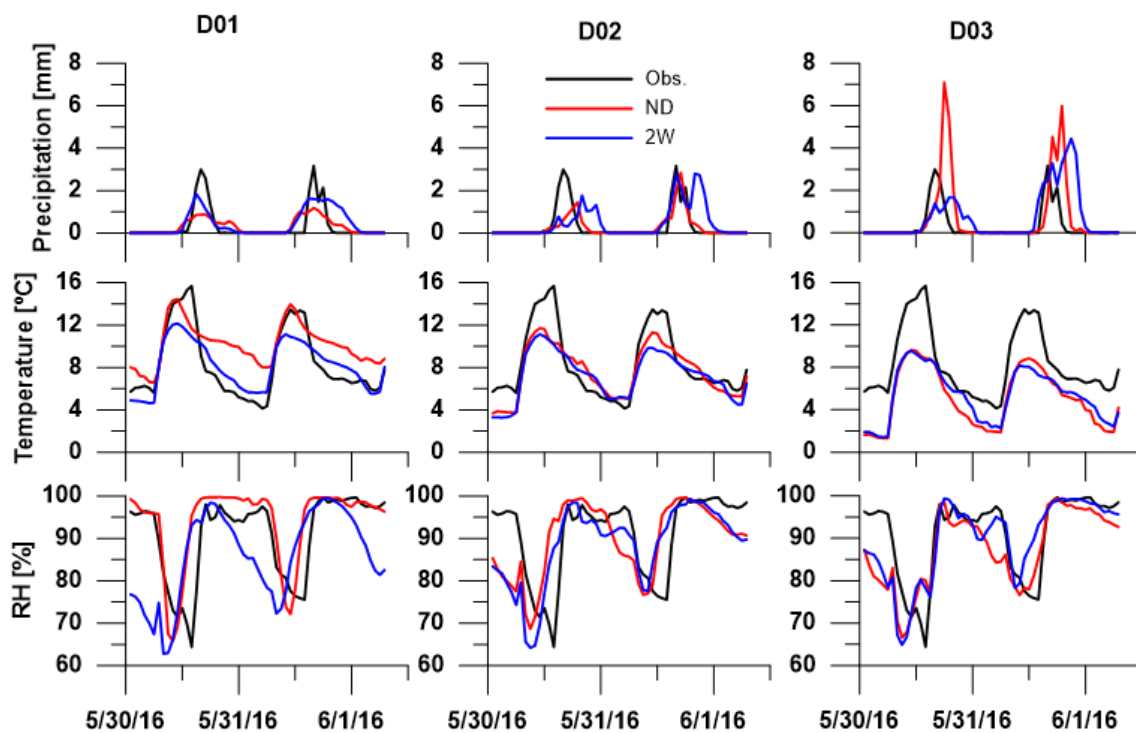


Figure 4 30/05/2016 event time series of precipitation, temperature and relative humidity, observed and downscaled by ND and 2W for D01, D02 and D03 from left to right

The advantages and disadvantages of 2W in terms of accuracy and computational efficiency have been reported by other studies. For instance, Fast et al., (2006) showed that a simulation with 2W nesting improved the representation of the urban and point sources within the coarse 12-km domain. Soriano [42] on the other hand, showed better performance in capturing precipitation by using ND rather than 2W. Thus the poor performance of ND obtained in the present study may be associated with perturbations to velocities and potential temperature from a nested fine grid to a coarse grid that degrade conservation properties (e.g., energy, entropy) required for accurate numerical solutions as well as possible mass non-conservation due to the interpolation errors and nonlinearity [35, 43]. In a broader context, downscaling precipitation errors are also controlled by the quality of the boundary forcing and the correlations between soils, temperature and transpiration in orographic terrains [12].

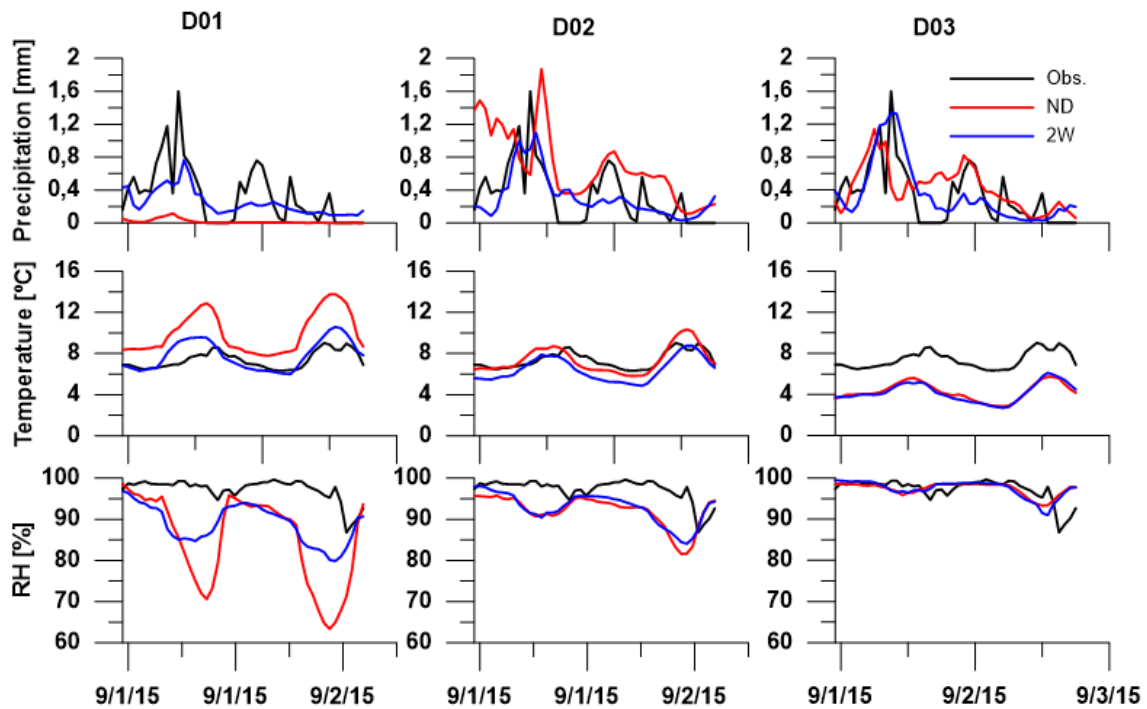


Figure 5 31/08/2015 event time series of precipitation, temperature and relative humidity, observed and downscaled by ND and 2W for D01, D02 and D03 from left to right

4.2. Timing and development of simulated events

4.2.1 Simulation of precipitation

In the last section 2W nesting showed better results than ND downscaling approach, especially on finer resolution. Therefore further analysis is conducted only to the 2W downscaled results. The comparison between the observed and modeled hourly precipitation was performed throughout the 60 and 48 hours of model run for the two events. Figure 6 presents the observed and modeled precipitation time series using the configurations described in Table 1 for both events, left 30/05/2016 and right 31/08/2015 for D01 to D03 from top to bottom. Each colored line represents one configuration.

For the 30/05/2016 event in D01, (Figure 6 Top-left), the first peak of precipitation is slightly captured in timing and amount by C5, C1 and C3. To a lesser extent it is captured by C4 and C2. However the second peak is slightly overestimated and the configurations C5 and C3 perform better than the others. For D02, (Figure 6 Center-left), on the first peak, the timing of the models do not match the observations and the amount is overestimated especially by C4 & C5. In 4 km resolution, (Figure 6 Bottom-left), the first peak is not captured and the second peak is very strongly overestimated especially by C5, C1 and C3. For the 31/08/2015 event (Figure 6 right), the observed precipitation is rather variable in time, thus capturing such evolution is expected to be difficult. In D01, (Figure 6 Top-right), the first two peaks are slightly underestimated by all configurations, and the following peak is only captured by C3 & C4. In 12km resolution C1, C2 & C5 capture only the first two peaks. C3 & C4 are not able to capture the whole event. In 4 km resolution C1, C2 & C5 only capture the first two peaks. However precipitation is overestimated by C3, all other configurations improve their performance by enhancing its resolution. These results show that downscaling improves the simulation of precipitation processes. In Figure 6 the precipitation varies



significantly among configurations. Also, C2 and C3 microphysics configurations are sensible to the choice of PBL, while the C5 shows higher variability of precipitation forecasts with respect to the choice of PBL parameterization.

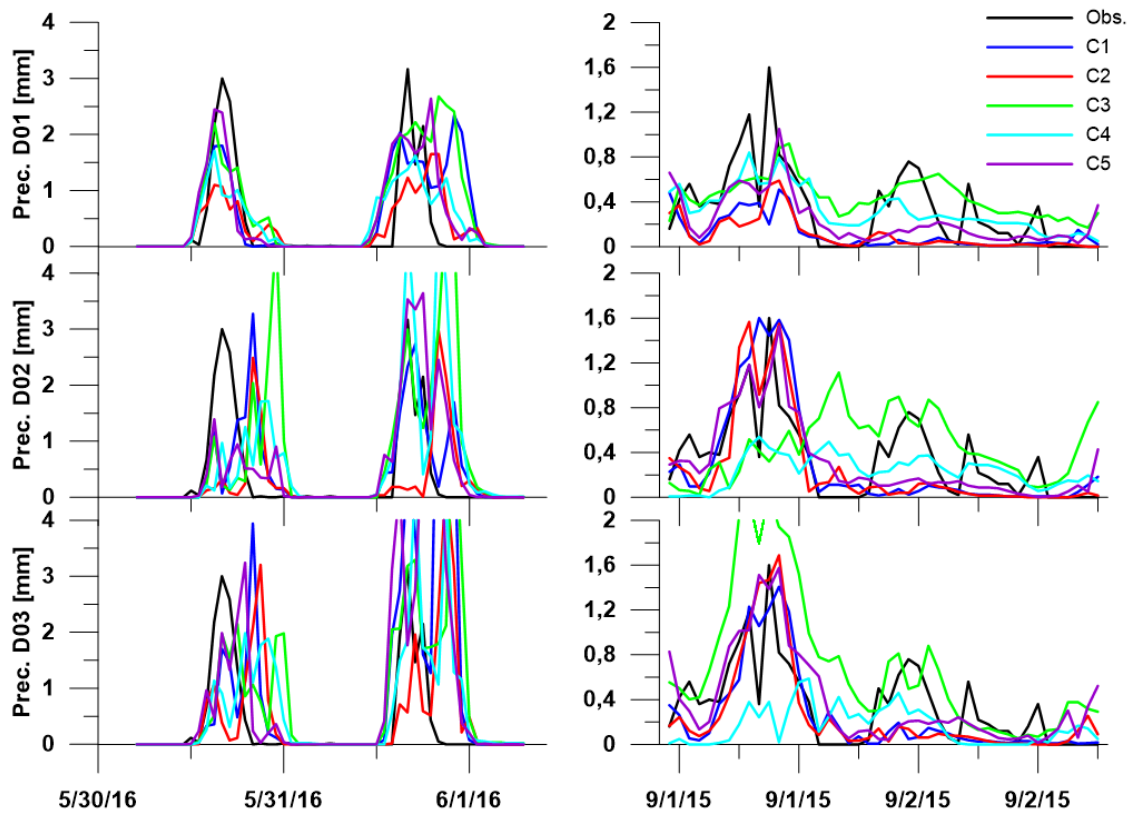


Figure 6 Precipitation time series for 30/05/2016 (left) and 31/08/2015 (right), for D01, D02 and D03 from top to bottom.

On the 30/05/2016 event (Figure 7 left) the evolution and timing is well forecasted by all the configurations across the three domains. For instance in D01 (Figure 7 top left) configurations start consistently the first sub event, however C1 and C5 present ca. 2 hours lag. For the second sub event all configurations start 3 to 4 hours earlier. Once again PBL overestimates precipitation. This is evident from the 36st hour on C1, C3 and C5. MYNN 2.5 scheme is more in concordance with the final cumulative value of precipitation, with a bias of +2 mm for C4 and -4 mm for C2. In D02 the development of the event fits the observations although the timing has a lag on the first sub event. For the second sub event all configurations with exception of C2 start at the same time, despite an overestimation of cumulative precipitation. In this domain C2 presents the poorest forecast. For D03 only C2 and C4 overestimate the precipitation on 5 and 12 mm respectively, meanwhile the other configurations overpass the 50 mm. On the finer grid the MYNN 2.5 PBL scheme is the more accurate representing the cumulative precipitation, despite some discrepancies on the sub events. As shown in Figure 7 during the no rain stage all the configurations have almost the same volume and lower bias. This is an indicator that the non-local PBL scheme has difficulties to forecast the last 24 hours. For the 31/08/2015 event the cumulative precipitation is shown in Figure 7. In D01 the difference between configurations with Thompson microphysics (C1&C2) and Ferrier microphysics (C3&C4) are evident. The former show lower values meanwhile the latter are more accurate. Nevertheless dynamics is kept until the first 18 hours of forecast. The YSU PBL scheme presents better performance with exception of C1. On D02 there is no change for the Ferrier microphysics scheme, however the dynamics and timing are limited with respect to D01. For the rest of the configurations



the dynamics, timing and the cumulative precipitation is near to the observations. In D03, C1, C2 and C5 have an appropriated representation of rainfall, but the development is adequate only during the first 18 hours. PBL scheme plays an important role with YSU showing the best performance. Contrarily, Jankov [44] show that PBL do not present key implications to precipitation products. Figure 7 indicates that most parameterization schemes overestimate the amount of rainfall. Furthermore, PBL schemes may result in the misallocation of high precipitation values, e.g. C4, similar to the results obtained for YSU by Weisman [11].

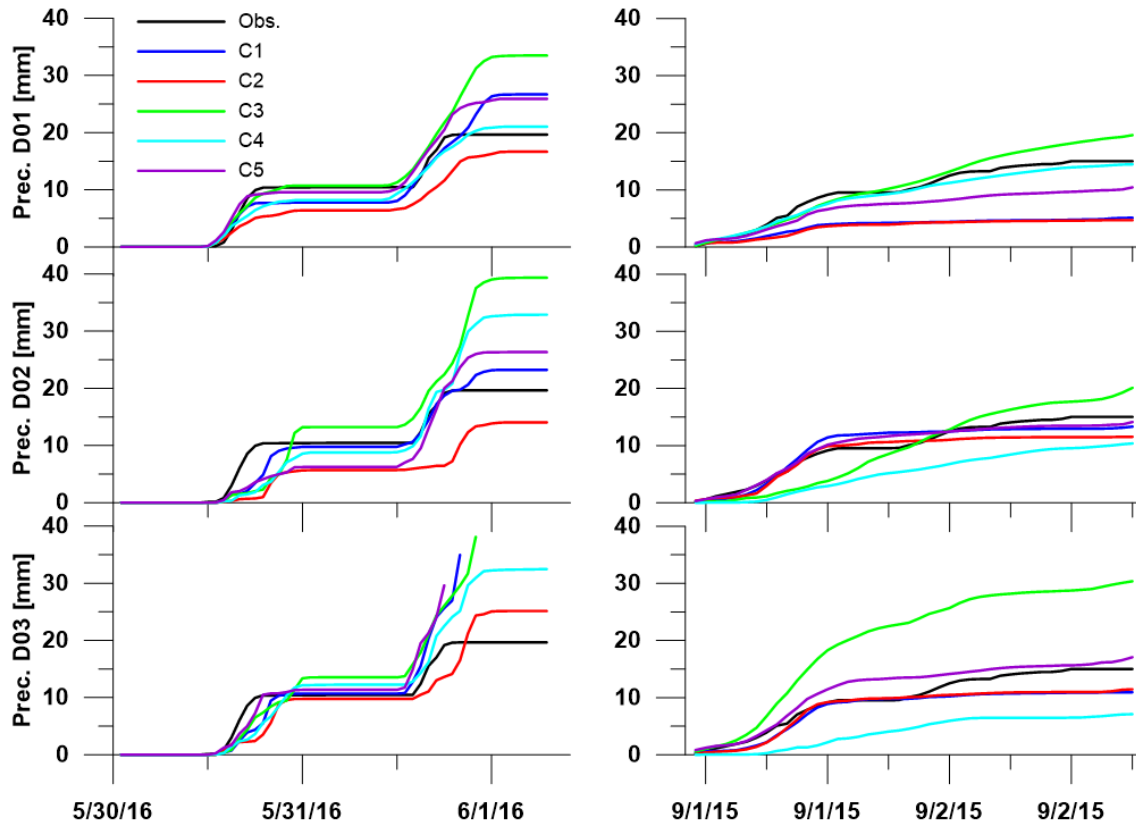


Figure 7 Cumulative precipitation time series for 30/05/2016 (left) and 31/08/2015 (right), for D01, D02 and D03 from top to bottom.

Figure 8 presents the Taylor diagrams for 30/05/2016 (left) and 31/08/2015 (right) events. Two arrows of the same color are the representation in the diagram from D01 to D02 and from D02 to D03 corresponding to the same configuration. For the 30/05/2016 event (Figure 8 left) C1 shows a good representation for 36 and 12 km resolution. However for 4 km resolution the standard deviation is strongly overestimated. C5 shows similar results. For C2 the correlation from 36 to 12 km decreases, and some improvement is achieved from 12 to 4 km resolution. However for C2 the best representation is on D01. For C3 the correlation from D01 to D02 decreases, and some improvement is shown from D02 to D03, although the standard deviation is overestimated in ca. 50%. The correlation of C4 from D01 to C02 and to C03 decreases consistently. These results indicate that the representation of the rainy season event on the inner domain with higher resolution is not well captured. Thus for a heavy precipitation event, all configurations present difficulties in modeling, in relation to timing, dynamics and volume. This may be due to the topographical control of precipitation [45].

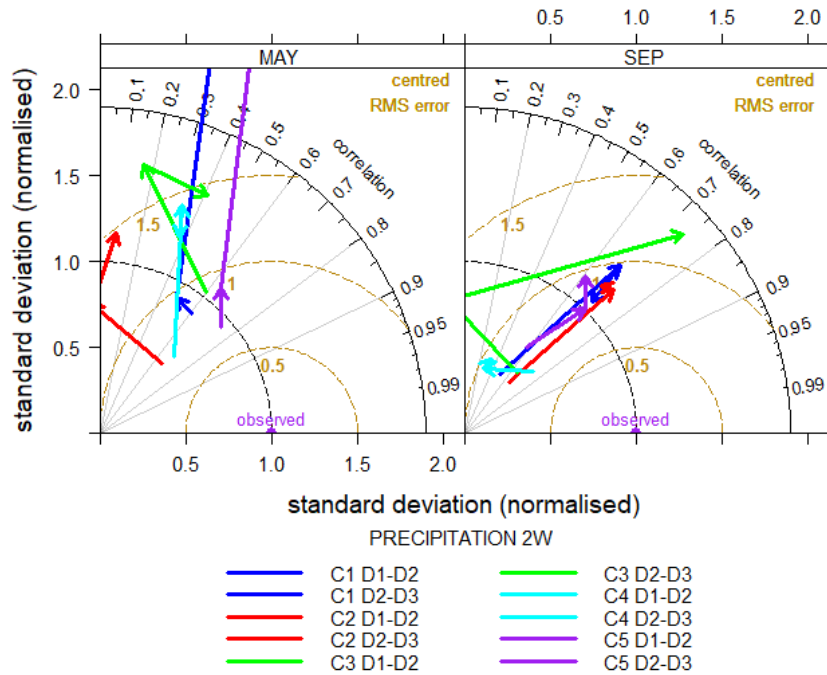


Figure 8 Taylor plots for the precipitation on both events across the three domains (end of the arrow indicate domain resolution improvement)

For the May 2016 event, the configurations C1, C2 and C5 show a better agreement with observations. Although C3 and C4 have a better performance in the inner domain this is not as good as for the first configurations. PBL scheme is YSU, however microphysics is different for all the configurations. For September the configurations C1, C2 and C5 show a better agreement with observations, C3 has a weaker performance in the inner domain but C4 has negative correlation and a bigger bias. Configurations C1 and C5 represent YSU scheme for PBL, however C5 microphysics is WSM 6 whereas C1 and C2 are Thompson scheme. On the inner domain both events are simulated with lower bias (+5mm for May and +-2 mm for September except for C1 and C2), but the timing and dynamics on September generates lags of one hour, and on the 30th May more than two hours. The development for May event is on concordance, however some overestimation is present on the second part of the event (42 hours of simulation). Nevertheless the bias of C2 and C3 are lower than the rest of configurations. The same effect is shown by Xu [46] where the bias in precipitation for forecast larger than 24 hours rise up to 20 mm. Overall, the C1, C3 and C5 configurations were superior with respect to the magnitudes of extremes for the event on May and configurations C1, C2 and C5 for the event on September with a positive or negative bias on the order of 10 to 15 mm.

4.2.2. Simulation of temperature

The analysis of the simulated temperature is important because it is related to the energy available for the atmospheric processes and may be, in conjunction with relative humidity a proxy of atmospheric instability [47]. Figure 9 presents the observed and modeled temperature time series using the configurations described in Table 1 for both events, left 30/05/2016 and right 31/08/2015. Each colored line represents one configuration.



Figure 9 left shows the May 2016 event forecasted temperature. For domain D01 there is an underestimation of about 2 to 4 °C during the day, and an overestimation of 1°C at nighttime. The evolution and timing of the event is in concordance with the observations for all the configurations. On D02 the daily temperature is underestimated but the bias is greater than in D01. The first night forecast has some perturbations with high and low variation across the night with positive bias, but for the second night up to 42 hours of forecast all configurations fall below the observations at the end of the 50th hour of forecast. The temperature on D03 is underestimated by all configurations, especially the midday peak.

On Figure 9-right the event of September 2015 is represented from top to bottom on the three domains. D01 shows an accurate representation of nighttime temperature. However during the day time the temperature is overestimated. The timing for the first day has an early start, and the peak of the day is located in the early morning. It should be observed that the double peak on the 02/09/2015 at 10H00 and 15H00, any configuration is able to represent. For D02 as in the event of May 2016 the nighttime drop of temperature is represented for this event. The evolution and timing are the same as for D01, but the bias increases to -2°C. D03 has a bias of -3°C which visually is prominent compared to D02 and D01. Surprisingly the timing is improved but it maintains a lag of 2 hours to the first peak of the forecast on all configurations. C1, C3 and C5 show a good representation of the second peak and C2 and C4 in a much lesser extend.

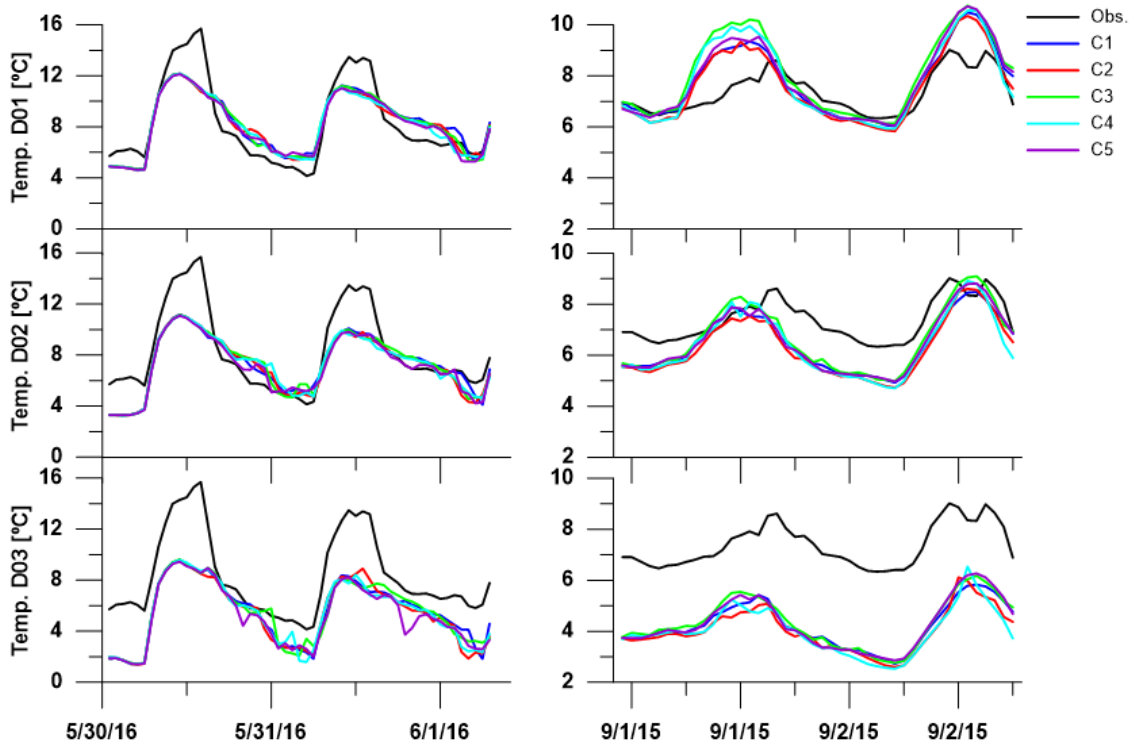


Figure 9 Temperature time series for 30/05/2016 (left) and 31/08/2015 (right), for D01, D02 and D03 from top to bottom.

Figure 10 presents the Taylor diagrams for temperature. The simulations of the 30/05/2016 event do not show a representative improvement from 36 to 12 to 4 km resolution. However it is important to highlight that all the configurations show similar temperature results. The simulation of the 31/08/2015 event, evaluated by the Taylor plot, shows improvements by enhancing the resolution. However, this diagram does not capture the cold bias shown by the time series presented in Figure 9.

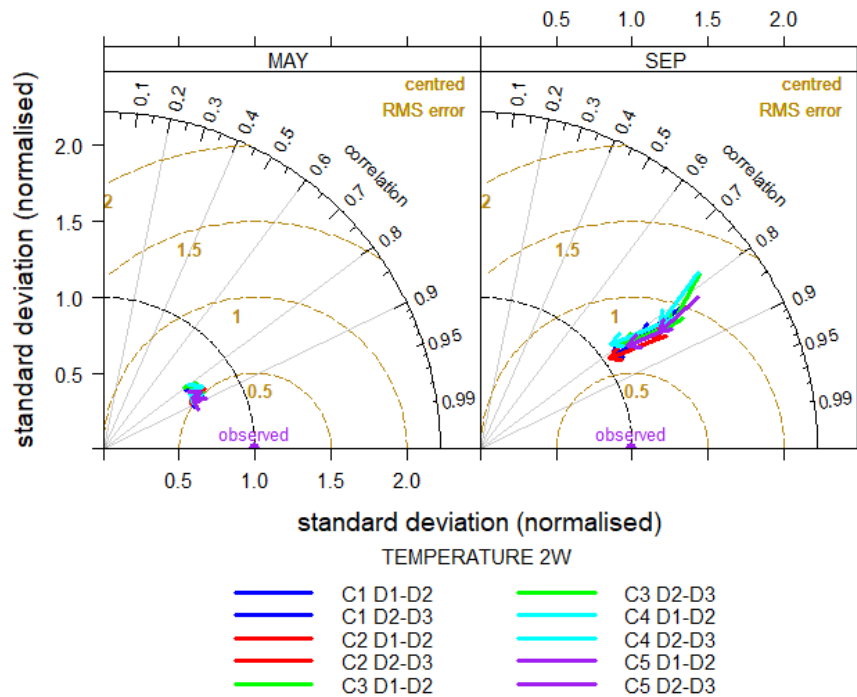


Figure 10 Temperature Taylor Diagram for the configurations at each Domain (the arrows indicate the development of resolution). Left and right, 30/05/2016 and 31/08/2015 event.

Summarizing the results of temperature, in D01 midday temperature is underestimated for the May-2016 event, in contrast to the September-2015 event where temperature is overestimated by ca. 2°C. This result is similar to Case, et al., (2008). They showed that the forecast of precipitation maintain colder bias on mountainous regions of about 2 Celsius degrees over the Florida Peninsula. It is interesting to observe that the downscaling procedure deteriorate the temperature simulation. With respect to the evolution of temperature, all configurations show some agreement. However there is a lag of almost 4 hours in the event of September-2015 for the first peak. Similar results with larger cold bias are reported by Xu [46] on the Tibetan Plateau. They suggest that the problem is a model deficit on the description of surface temperature on high terrains areas. Also Coniglio [36] address the large negative temperature errors to the inability of the model physical parameterizations to properly predict the evolution of the convective clouds and their effects on the temperature and moisture profiles in the PBL during the day.

4.2.3 Simulation of relative humidity

Relative humidity at 2m is an important key to understand the saturation of vapor in the atmosphere [49]. A good representation of observed relative humidity may be a proxy of a good representation of precipitation. In Figure 11 the observed and modeled relative humidity using the configurations described in Table 1 for both events, left 30/05/2016 and right 31/08/2015 for D01 to D03 from top to bottom are presented.

For the 30/05/2016 event, Figure 11 left, the relative humidity results on D01 show a lag of midday drop. The evolution isn't well simulated during the nights. The bias generated on this domain is lower than 3% at most, but there is misrepresentation of the nighttime hours. On D02 the bias remains as in D01 and the nighttime hours



variability for 31/05/2016 is greater for C1, C2 and C5, configurations with microphysics of 5 and 6 class variables. Meanwhile C2 and C4 use a simpler 4 class variables. During the day 01/06/2016 this effect is damped. For D03 some evolution is shown with exception of nighttime hours. The morning of 01/06/2016 is better represented and the timing of the nocturnal cycle is also a remarkable improvement of the microphysics, which is independent of the PBL.

For the 31/08/2015 event (Figure 11 right), the representation of RH for D01 has a poor performance in evolution, timing and bias for the whole event. The performance is lower during the day than during the night. Ferrier microphysics (C3&C4) has a lower efficiency than the rest of the configurations. On D02 the evolution is better than D01, the lag stills on the same amount as in D01 but the bias is reduced. Domain D03 has a better agreement with the observations than D01&D02 especially in the evolution of the event. There is an overestimation of RH during the day. In some cases it reaches 100% of RH as in C1 and C2. The bias in this domain is reduced to +- 1% in the extremes. The lag on the midday of the forecast is of 1/2 hours for C4/C1 to C5 respectively. For the 02/09/2015 C2 and C4 are the more accurate configurations to the minimum value of RH, which are configurations with different Microphysics but the same PBL scheme.

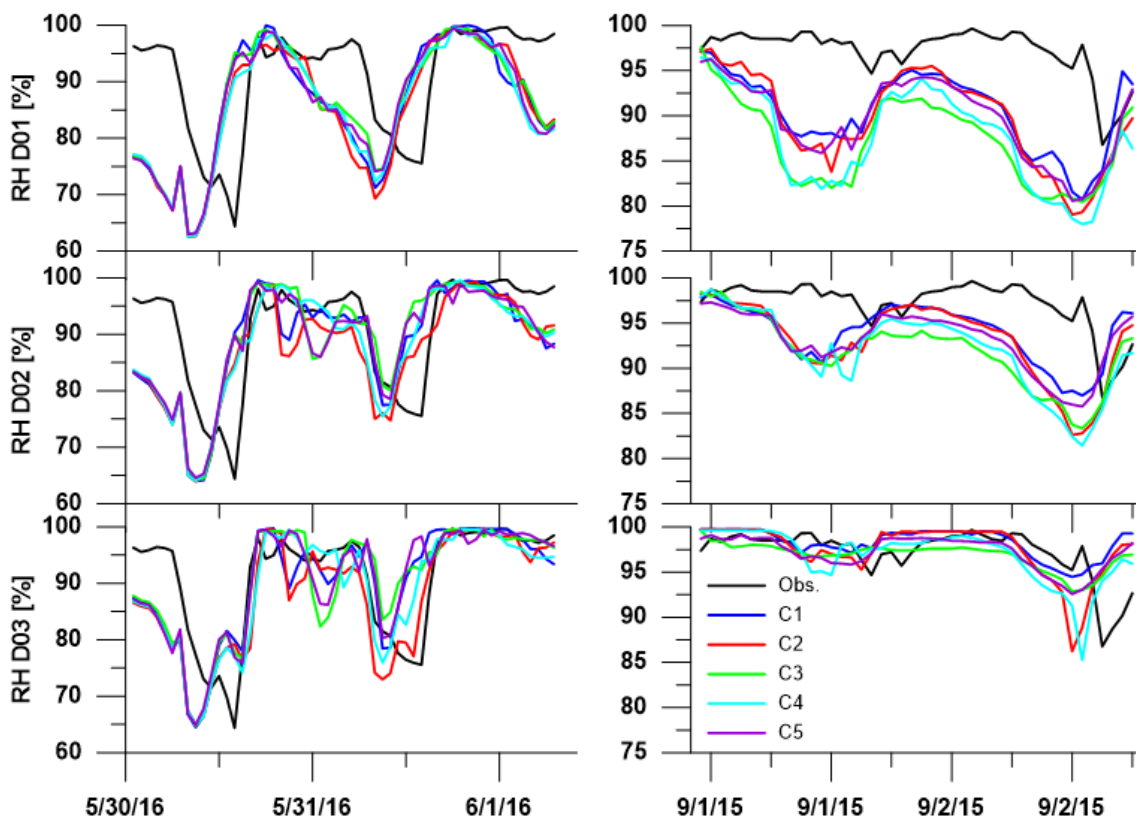


Figure 11 RH time series of WRF configurations vs Observed data

Figure 12 shows the Taylor diagram of the configurations for RH at 30/05/2016 and 31/08/2015, left & right respectively. For May-2016 the increase in resolution produces an increase in performance. The leading configurations are C4, C3 and C1. In the case of September-2015 D02 has a better representation with respect to D01 and D03, with exception of C1 and C5.

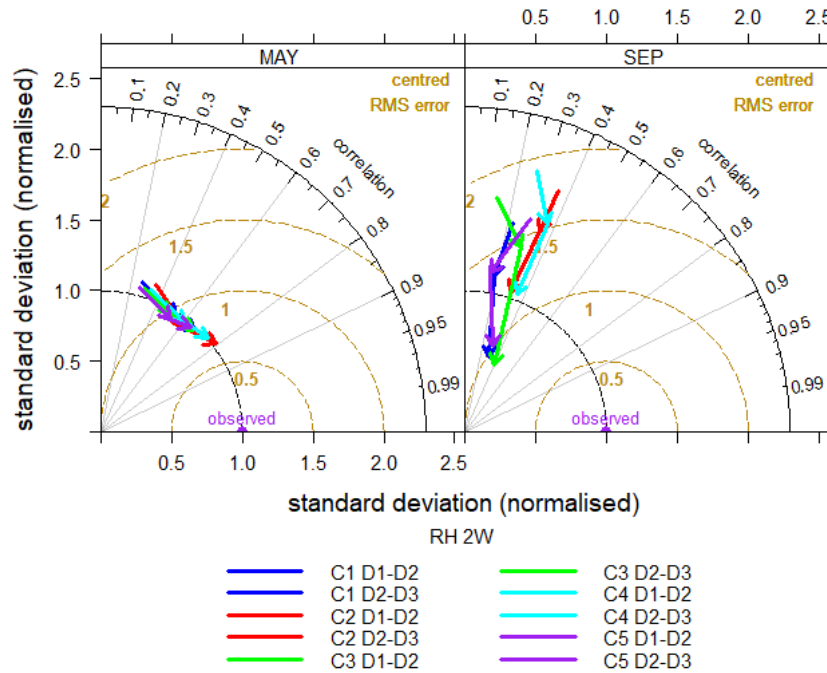


Figure 12 RH Taylor Diagram for the configurations at each Domain (the arrows indicate the develop of resolution)

The forecast of RH has a considerable negative bias especially for the dry season event. In general with increasing resolution the forecast improves. There is a lack of ability to represent the nocturnal pattern for all the configurations. C5 shows one of the worst performances in the event of May-2016 for all domains. In September-2015 the representation of the evolution of RH is limited especially in the outer domains. Clearly the combination of the microphysics and the PBL help to achieve better RH forecasting. Non-local PBL schemes as YSU tend to generate dry conditions near the ground, meanwhile the local scheme has a better performance with a lower dry bias for the simulation. Cheng [50] and Coniglio [51] show similar results in relative humidity representation, where YSU has a dryer bias on the first 1.5 km over the continental United States of America (US) leading to a bad mixing ratios on the PBL, meanwhile in the Western US the RH has a negative bias which is not correspondent to the negative temperature bias.

5. Conclusions

In the present study, the impact on precipitation, temperature and relative humidity forecasting of two sub-grid parameterization schemes, microphysics and planetary boundary layer (PBL), is evaluated. The results were compared for three resolutions (e.g. 4km, 12 km and 36 km) in two nested domains. The state of the art model Weather Research and Forecasting model (WRF) driven by Global Forecasting System data (GFS) was used. The study is conducted in the Quinuas Catchment, 94 km², in two events, one in the rainy season and the other in the dry season, to account for differentiated synoptic conditions.

The configurations Thompson&YSU, Thompson&MYNN, Ferrier&YSU, Ferrier&MYNN, and WSM&YSU were evaluated for microphysics & PBL, respectively. The results indicate that the forecasting, especially of precipitation, is sensitive to the PBL scheme



depending on the season. This impact is more evident on lower grid resolutions e.g. 36 & 12 km. Also, PBL is sensitive to higher resolution, improving likewise the timing of the precipitation and the development of temperature and relative humidity during the event. The PBL parameterization is in dependence of the microphysics scheme used. For instance MYNN with Thompson has a better performance for the rainy season event, whereas YSU with Thompson is better for the dry season event. Consistently, the microphysics scheme is second to the PBL parameterization selection in importance. Microphysics WSM6 does not show good simulations. However, it is interesting to highlight that, in the inner domain, the results of both PBL's approaches converge to very similar results in precipitation, temperature and relative humidity. Further studies based on more physical parameterizations should be conducted in this area to analyze in a deeper way the climatology and the forces driving convective and orographic precipitation.

6. Acknowledges

This research was funded by the Central Research Office (DIUC) of the University of Cuenca in the framework of the project "Evaluación del riesgo de inundación en el río Santa Bárbara". This manuscript is an outcome of UCuenca's Master in Ecohydrology. The authors thank the Department of Hydric Resources and Environmental Sciences (IDRHICA) of the University of Cuenca to provide the data for the work. Special thanks are to the personnel of the University that participated in the work: Juan Saenz and Pablo Contreras.

7. References

1. M.R. Allen and W.J. Ingram: "Constraints on future changes in climate and the hydrologic cycle." *Nature*. vol. 419, no. 6903, pp. 224–232, 2002.
2. R. Misumi, V.A. Bell, and R.J. Moore: "River flow forecasting using a rainfall disaggregation model incorporating small-scale topographic effects." *Meteorol. Appl.* vol. 8, no. 3, pp. S135048270100305X, 2001.
3. P. Bauer-Gottwein, I.H. Jensen, R. Guzinski, G.K.T. Bredtoft, S. Hansen, and C.I. Michailovsky: "Operational river discharge forecasting in poorly gauged basins: the Kavango River basin case study." *Hydrol. Earth Syst. Sci.* vol. 19, no. 3, pp. 1469–1485, 2015.
4. C.J.A. Bradshaw, N.S. Sodhi, K.S.-H. Peh, and B.W. Brook: "Global evidence that deforestation amplifies flood risk and severity in the developing world." *Glob. Chang. Biol.* vol. 13, no. 11, pp. 2379–2395, 2007.
5. K.J. Beven: "On hypothesis testing in hydrology." 2001.
6. Z.-Y. Yin, X. Zhang, X. Liu, M. Colella, X. Chen, Z.-Y. Yin, X. Zhang, X. Liu, M. Colella, and X. Chen: "An Assessment of the Biases of Satellite Rainfall Estimates over the Tibetan Plateau and Correction Methods Based on Topographic Analysis." *J. Hydrometeorol.* vol. 9, no. 3, pp. 301–326, 2008.
7. L. Ma, T. Zhang, O.W. Frauenfeld, B. Ye, D. Yang, and D. Qin: "Evaluation of precipitation from the ERA-40, NCEP-1, and NCEP-2 Reanalyses and CMAP-1, CMAP-2, and GPCP-2 with ground-based measurements in China." *J. Geophys. Res.* vol. 114, no. D9, pp. D09105, 2009.
8. J.E. Box, D.H. Bromwich, and L. Bai: "Greenland ice sheet surface mass balance 1991–2000: Application of Polar MM5 mesoscale model and in situ data." *J. Geophys. Res.* vol. 109, no. D16, pp. D16105, 2004.
9. J.E. Box, D.H. Bromwich, B.A. Veenhuis, L.-S. Bai, J.C. Stroeve, J.C. Rogers, K. Steffen, T. Haran, S.-H. Wang, J.E. Box, D.H. Bromwich, B.A. Veenhuis, L.-S. Bai, J.C. Stroeve, J.C. Rogers, K. Steffen, T. Haran, and S.-H. Wang: "Greenland Ice Sheet Surface Mass Balance Variability (1988–2004) from Calibrated Polar MM5 Output*." *J. Clim.* vol. 19, no. 12, pp. 2783–2800, 2006.
10. M.S. Bukovsky and D.J. Karoly: "Precipitation simulations using WRF as a nested regional climate model." *J. Appl. Meteorol. Climatol.* vol. 48, no. 10, pp. 2152–2159, 2009.
11. M.L. Weisman, C. Davis, W. Wang, K.W. Manning, J.B. Klemp, M.L. Weisman, C. Davis, W. Wang, K.W. Manning, and J.B. Klemp: "Experiences with 0–36-h Explicit Convective Forecasts



- with the WRF-ARW Model.” *Weather Forecast*. vol. 23, no. 3, pp. 407–437, 2008.
12. K. Warrach-Sagi, T. Schwitalla, V. Wulfmeyer, and H.-S. Bauer: “Evaluation of a climate simulation in Europe based on the WRF–NOAH model system: precipitation in Germany.” *Clim. Dyn.* vol. 41, no. 3–4, pp. 755–774, 2013.
 13. G. Zängl: “To what extent does increased model resolution improve simulated precipitation fields? A case study of two north-Alpine heavy-rainfall events.” *Meteorol. Zeitschrift*. vol. 16, no. 5, pp. 571–580, 2007.
 14. D.G. Hahn, S. Manabe, D.G. Hahn, and S. Manabe: “The Role of Mountains in the South Asian Monsoon Circulation.” *J. Atmos. Sci.* vol. 32, no. 8, pp. 1515–1541, 1975.
 15. M.L.M. Scheel, M. Rohrer, C. Huggel, D. Santos Villar, E. Silvestre, and G.J. Huffman: “Evaluation of TRMM Multi-satellite Precipitation Analysis (TMPA) performance in the Central Andes region and its dependency on spatial and temporal resolution.” *Hydrol. Earth Syst. Sci.* vol. 15, pp. 2649–2663, 2011.
 16. E. Ward, W. Buytaert, L. Peaver, and H. Wheeler: “Evaluation of precipitation products over complex mountainous terrain: A water resources perspective.” *Adv. Water Resour.* vol. 34, no. 10, pp. 1222–1231, 2011.
 17. X. Zhou, A. Beljaars, Y. Wang, B. Huang, C. Lin, Y. Chen, and H. Wu: “Evaluation of WRF Simulations With Different Selections of Subgrid Orographic Drag Over the Tibetan Plateau.” *J. Geophys. Res. Atmos.* vol. 122, no. 18, pp. 9759–9772, 2017.
 18. W. Buytaert, M. Vuille, A. Dewulf, R. Urrutia, A. Karmalkar, and R. Céleri: “Uncertainties in climate change projections and regional downscaling in the tropical Andes: implications for water resources management.” *Hydrol. Earth Syst. Sci.* vol. 14, no. 7, pp. 1247–1258, 2010.
 19. R. Celleri, P. Willems, W. Buytaert, and J. Feyen: “Space–time rainfall variability in the Paute basin, Ecuadorian Andes.” *Hydrol. Process.* vol. 21, no. 24, pp. 3316–3327, 2007.
 20. D.E. Mora, L. Campozano, F. Cisneros, G. Wyseure, and P. Willems: “Climate changes of hydrometeorological and hydrological extremes in the Paute basin, Ecuadorean Andes.” *Hydrol. Earth Syst. Sci.* vol. 18, no. 2, pp. 631–648, 2014.
 21. L. Campozano, R. Céleri, K. Trachte, J. Bendix, E. Samaniego, and E. Samaniego: “Rainfall and Cloud Dynamics in the Andes: A Southern Ecuador Case Study.” *Adv. Meteorol.* vol. 2016, pp. 1–15, 2016.
 22. A. Ochoa, L. Campozano, E. Sánchez, R. Gualán, and E. Samaniego: “Evaluation of downscaled estimates of monthly temperature and precipitation for a Southern Ecuador case study.” *Int. J. Climatol.* vol. 36, no. 3, pp. 1244–1255, 2016.
 23. K. Trachte, R. Rollenbeck, and J. Bendix: “Nocturnal convective cloud formation under clear-sky conditions at the eastern Andes of south Ecuador.” *J. Geophys. Res.* vol. 115, no. D24, pp. D24203, 2010.
 24. P.B. Cerlini, K.A. Emanuel, and E. Todini: “Orographic effects on convective precipitation and space-time rainfall variability: preliminary results.” *Hydrol. Earth Syst. Sci. Discuss.* vol. 9, no. 4, pp. 285–299, 2005.
 25. M. Nakanishi and H. Niino: “AN IMPROVED MELLOR – YAMADA LEVEL - 3 MODEL : ITS NUMERICAL STABILITY AND APPLICATION TO A REGIONAL PREDICTION OF ADVECTION FOG.” *Bound. - Layer Meteorol.* vol. 119, pp. 397–407, 2006.
 26. J.J. Ruiz, C. Saulo, and J. Nogués-Paegle: “WRF Model Sensitivity to Choice of Parameterization over South America: Validation against Surface Variables.” *Mon. Weather Rev.* vol. 138, no. 8, pp. 3342–3355, 2010.
 27. S.-Y. Hong, J. Dudhia, S.-H. Chen, S.-Y. Hong, J. Dudhia, and S.-H. Chen: “A Revised Approach to Ice Microphysical Processes for the Bulk Parameterization of Clouds and Precipitation.” *Mon. Weather Rev.* vol. 132, no. 1, pp. 103–120, 2004.
 28. Y.V.R. Rao, H.R. Hatwar, A.K. Salah, and Y. Sudhakar: “An Experiment Using the High Resolution Eta and WRF Models to Forecast Heavy Precipitation over India.” *Pure Appl. Geophys.* vol. 164, no. 8–9, pp. 1593–1615, 2007.
 29. M. Rajeevan, A. Kesarkar, S.B. Thampi, T.N. Rao, B. Radhakrishna, and M. Rajasekhar: “Sensitivity of WRF cloud microphysics to simulations of a severe thunderstorm event over Southeast India.” *Ann. Geophys.* vol. 28, pp. 603–619, 2010.
 30. M. Vuille, R.S. Bradley, F. Keimig, M. Vuille, R.S. Bradley, and F. Keimig: “Climate Variability in the Andes of Ecuador and Its Relation to Tropical Pacific and Atlantic Sea Surface Temperature Anomalies.” *J. Clim.* vol. 13, no. 14, pp. 2520–2535, 2000.
 31. J.S. Kain: “The Kain–Fritsch Convective Parameterization: An Update.” *J. Appl. Meteorol.* pp. 170–181, 2003.
 32. J.A. Milbrandt, M.K. Yau, J.A. Milbrandt, and M.K. Yau: “A Multimoment Bulk Microphysics



- Parameterization. Part II: A Proposed Three-Moment Closure and Scheme Description.” *J. Atmos. Sci.* vol. 62, no. 9, pp. 3065–3081, 2005.
33. M.L. Weisman, C. Davis, W. Wang, K.W. Manning, and J.B. Klemp: “Experiences with 0–36-h Explicit Convective Forecasts with the WRF-ARW Model.” *Weather Forecast.* vol. 23, no. 3, pp. 407–437, 2008.
 34. E. Gego, C. Hogrefe, G. Kallos, A. Voudouri, J.S. Irwin, and S.T. Rao: “Examination of model predictions at different horizontal grid resolutions.” *Environ. Fluid Mech.* vol. 5, no. 1–2, pp. 63–85, 2005.
 35. J.D. Fast, W.I. Gustafson, R.C. Easter, R.A. Zaveri, J.C. Barnard, E.G. Chapman, G.A. Grell, and S.E. Peckham: “Evolution of ozone, particulates, and aerosol direct radiative forcing in the vicinity of Houston using a fully coupled meteorology-chemistry-aerosol model.” *J. Geophys. Res.* vol. 111, no. D21, pp. D21305, 2006.
 36. M.C. Coniglio, K.L. Elmore, J.S. Kain, S.J. Weiss, M. Xue, and M.L. Weisman: “Evaluation of WRF Model Output for Severe Weather Forecasting from the 2008 NOAA Hazardous Weather Testbed Spring Experiment.” *Weather Forecast.* vol. 25, no. 2, pp. 408–427, 2010.
 37. A. Ochoa, L. Pineda, P. Crespo, and P. Willems: “Evaluation of TRMM 3B42 precipitation estimates and WRF retrospective precipitation simulation over the Pacific–Andean region of Ecuador and Peru.” *Hydrol. Earth Syst. Sci.* vol. 18, no. 8, pp. 3179–3193, 2014.
 38. K.E. Taylor: “Summarizing multiple aspects of model performance in a single diagram.” *J. Geophys. Res. Atmos.* vol. 106, no. D7, pp. 7183–7192, 2001.
 39. S. Joseph, A.K. Sahai, and B.N. Goswami: “Boreal summer intraseasonal oscillations and seasonal Indian monsoon prediction in DEMETER coupled models.” *Clim. Dyn.* vol. 35, no. 4, pp. 651–667, 2010.
 40. P.A. Jiménez, J.F. González-Rouco, E. García-Bustamante, J. Navarro, J.P. Montávez, J.V.-G. de Arellano, J. Dudhia, A. Muñoz-Roldan, P.A. Jiménez, J.F. González-Rouco, E. García-Bustamante, J. Navarro, J.P. Montávez, J.V.-G. de Arellano, J. Dudhia, and A. Muñoz-Roldan: “Surface Wind Regionalization over Complex Terrain: Evaluation and Analysis of a High-Resolution WRF Simulation.” *J. Appl. Meteorol. Climatol.* vol. 49, no. 2, pp. 268–287, 2010.
 41. G. Roux, Y. Liu, L.D. Monache, R.-S. Sheu, and T.T. Warner: “Verification of high resolution WRF-RTFDDA surface forecasts over mountains and plains.” Proceedings of the 10th WRF Users’ Workshop (2009).
 42. C. Soriano, O. Jorba, and J.M. Baldasano: “One-Way Nesting Versus Two-Way Nesting : Does It Really Make a Difference?” *Unkn. J.* 2004.
 43. T. Schwitalla, H.-S. Bauer, V. Wulfmeyer, and F. Aoshima: “High-resolution simulation over central Europe: assimilation experiments during COPS IOP 9c.” *Q. J. R. Meteorol. Soc.* vol. 137, no. S1, pp. 156–175, 2011.
 44. I. Jankov, W. a. Gallus, M. Segal, B. Shaw, and S.E. Koch: “The Impact of Different WRF Model Physical Parameterizations and Their Interactions on Warm Season MCS Rainfall.” *Weather Forecast.* vol. 20, no. 2001, pp. 1048–1060, 2005.
 45. E.H. Berbery and E.A. Collini: “Springtime Precipitation and Water Vapor Flux over Southeastern South America.” *Mon. Weather Rev.* vol. 128, no. 5, pp. 1328–1346, 2000.
 46. J. Xu, S. Rugg, L. Byerle, Z. Liu, J. Xu, S. Rugg, L. Byerle, and Z. Liu: “Weather Forecasts by the WRF-ARW Model with the GSI Data Assimilation System in the Complex Terrain Areas of Southwest Asia.” *Weather Forecast.* vol. 24, no. 4, pp. 987–1008, 2009.
 47. Y.R. Jauregui and K. Takahashi: “Simple physical-empirical model of the precipitation distribution based on a tropical sea surface temperature threshold and the effects of climate change.” *Clim. Dyn.* pp. 1–21, 2017.
 48. J.L. Case, W.L. Crosson, S. V. Kumar, W.M. Lapenta, and C.D. Peters-Lidard: “Impacts of High-Resolution Land Surface Initialization on Regional Sensible Weather Forecasts from the WRF Model.” *J. Hydrometeorol.* vol. 9, no. 6, pp. 1249–1266, 2008.
 49. J. Milovac, K. Warrach-Sagi, A. Behrendt, F. Späth, J. Ingwersen, and V. Wulfmeyer: “Investigation of PBL schemes combining the WRF model simulations with scanning water vapor differential absorption lidar measurements.” *J. Geophys. Res. Atmos.* vol. 121, no. 2, pp. 624–649, 2016.
 50. W.Y.Y. Cheng and W.J. Steenburgh: “Evaluation of Surface Sensible Weather Forecasts by the WRF and the Eta Models over the Western United States.” *Weather Forecast.* vol. 20, no. 5, pp. 812–821, 2005.
 51. M.C. Coniglio, J. Correia, P.T. Marsh, and F. Kong: “Verification of Convection-Allowing WRF Model Forecasts of the Planetary Boundary Layer Using Sounding Observations.” *Weather Forecast.* vol. 28, no. 3, pp. 842–862, 2013.